Received: 18 August 2017 | Revised: 15 December 2017 | Accepted: 16 January 2018

DOI: 10.1002/term.2646

RESEARCH ARTICLE

WILEY

Generation of full-thickness skin equivalents using hair follicle-derived primary human keratinocytes and fibroblasts

Anna Löwa[1] | Annika Vogt[2] | Sabine Kaessmeyer[3] | Sarah Hedtrich[1]

[1] Institute for Pharmacy, Pharmacology and Toxicology, Freie Universität Berlin, Berlin, Germany

[2] Experimental Research Unit Clinical Research Center for Hair and Skin Sciences, Charité Universitätsmedizin Berlin, Berlin, Germany

[3] Department of Veterinary Medicine, Institute for Veterinary Anatomy, Freie Universität Berlin, Berlin, Germany

Correspondence
Sarah Hedtrich, Institute for Pharmacy, Pharmacology and Toxicology, Freie Universität Berlin, Königin-Luise-Str. 2-4, 14195 Berlin, Germany.
Email: sarah.hedtrich@fu-berlin.de

Funding information
BMBF Graduate School BB3R, Grant/Award Number: 031A262A

Abstract

Skin equivalents are increasingly used as human-based test systems for basic and preclinical research. Most of the established skin equivalents are composed of primary keratinocytes and fibroblasts, isolated either from excised human skin or juvenile foreskin following circumcisions. Although the potential of hair follicle-derived cells for the generation of skin equivalents has been shown, this approach normally requires microdissections from the scalp for which there is limited subject compliance or ethical approval. In the present study, we report a novel method to isolate and cultivate keratinocytes and fibroblasts from plucked hair follicles that were then used to generate skin equivalents. The procedure is non-invasive, inflicts little-pain, and may allow easy access to patient-derived cells without taking punch biopsies. Overall, minor differences in morphology, ultrastructure, expression of important structural proteins, or barrier function were observed between skin equivalents generated from hair follicle-derived or interfollicular keratinocytes and fibroblasts. Interestingly, improved basal lamina formation was seen in the hair follicle-derived skin equivalents. The presented method here allows easy and non-invasive access to keratinocytes and fibroblasts from plucked hair follicles that may be useful particularly for the generation of skin disease equivalents.

KEYWORDS

hair follicle, interfollicular keratinocytes and fibroblasts, outer rooth sheath, skin equivalents

1 | INTRODUCTION

Over the last decade, great efforts have been made in tissue engineering to develop organotypic models of human organs that accurately replicate structural and functional aspects found *in vivo*, and which could be used as alternative methods to animal testing. The increasing recognition that animal models often provide low predictive power for the human situation has further promoted the development of organ models (Leist & Hartung, 2013; Perrin, 2014; Seok et al., 2013). Significant progress has also been made in the development of human-based skin equivalents (Amelian, Wasilewska, Megias, & Winnicka, 2017; Ramata-Stunda, Boroduskis, Vorobjeva, & Ancans, 2013). These can be broadly characterised as either epidermal or full-thickness (FT) skin equivalents. Unlike epidermal equivalents, FT skin equivalents possess a dermal compartment that enables cellular crosstalk between keratinocytes and fibroblasts. Skin equivalents are either generated according to in-house protocols or can be purchased commercially. Commercial examples include EpiDerm® (MatTek, Ashland, MA) or SkinEthic® (SkinEthic laboratories, Nice, France), both of which are validated epidermal models for skin irritation and corrosion testing (OECD, 2016). Furthermore, skin equivalents are increasingly recognised as valuable models for preclinical research and basic science (Hönzke et al., 2016; van Smeden, Janssens, Gooris, & Bouwstra, 2014). They are conventionally generated from primary human keratinocytes and fibroblasts, isolated from either excised human skin or juvenile foreskin following circumcisions, or from keratinocyte cell lines (Reijnders et al., 2015). However, these approaches have clear limitations when aiming for the cultivation of patient-derived cells. Here, skin biopsies need to be taken by an invasive protocol that can result in discomfort and scar formation. Hence, patient compliance is poor.

Recently, the human hair follicle and its stem cell reservoir have received growing attention due to their potential for applications in the field of regenerative medicine (Mistriotis & Andreadis, 2013; Schembri, Scerri, & Ayers, 2013). The hair follicle contains a variety of cellular components: epithelial cells from the hair matrix and the

Abbreviations: CK, cytokeratin; HFDF, hair follicle-derived fibroblast; HFDK, hair follicle-derived keratinocyte; IL, interleukin; NHDF, normal human dermal fibroblast; NHK, normal human epithelial keratinocyte; ORS, outer root sheath

bulge region, the outer root sheath (ORS) in particular, mesenchymal cells from the dermal papilla and dermal sheath, plus several pools of epithelial, mesenchymal, and melanocyte stem cells (McElwee & Sinclair, 2008; Paus & Cotsarelis, 1999; Rompolas & Greco, 2014). The majority of the epithelial structures from the hair follicle remain attached after plucking (Gho, Braun, Tilli, Neumann, & Ramaekers, 2004). The feasibility of culturing undifferentiated keratinocytes isolated from the remaining ORS of plucked hair follicles (Limat & Noser, 1986; Weterings, Vermorken, & Bloemendal, 1981), and the formation of epidermal and FT models from these (Guiraud et al., 2014; Lenoir, Bernard, Pautrat, Darmon, & Shroot, 1988; Limat et al., 1991; Nakano et al., 2016) has already been demonstrated. However, there are few examples of the use of hair follicle-derived fibroblasts for the generation of FT skin equivalents (Cho, Bae, Kim, Im Na, & Park, 2004; Higgins et al., 2017). In these studies, fibroblast isolation was only possible with surgical microdissection of hair follicles, a step that greatly limits the feasibility of this approach. The ability to generate autologous FT skin equivalents from co-cultivated fibroblasts and keratinocytes derived from the same donor/patient without requiring invasive procedures would greatly improve patient compliance and facilitate these approaches. Hence, in the present study, we report a method to isolate primary human fibroblasts and keratinocytes from plucked hair follicles, offering a fully non-invasive technique to generate FT skin equivalents. The hair follicle-derived cells were comprehensively characterised with thorough comparisons to keratinocytes, fibroblasts, and skin equivalents derived from interfollicular skin cells.

2 | MATERIALS AND METHODS

2.1 | Isolation and cultivation of hair follicle-derived keratinocytes and fibroblasts

Ten to fifteen hair follicles were plucked from the scalp of healthy volunteers (age between 20 and 30, with ethical approval, EA1/345/14). Follicles in the anagen growth phase were identified based on the presence of an intact epithelial ORS as examined under an inverted microscope (Figure S1A). The distal keratinised hair shaft was cut off and immersed 4 times in Dulbecco's modified Eagle's medium (DMEM, Sigma-Aldrich, Germany) buffered with 25 nM HEPES (Life Technologies, Darmstadt, Germany) supplemented with 400 U/ml penicillin, 400 µg/ml streptomycin, and 250 ng/ml amphotericin B (Sigma-Aldrich, Munich, Germany; Aasen & Izpisua Belmonte, 2010; Limat, Hunziker, Boillat, Bayreuther, & Noser, 1989). The hair follicles were then placed on cell culture inserts (Corning, Costar 3450, USA) previously coated with postmitotic 3T3-J2 fibroblasts (3×10^4 cells/cm^2) on their basal side and cultivated submerged in a defined outgrowth medium consisting of 10% fetal bovine serum (FBS, Biochrom, Berlin, Germany), 5 µg/ml insulin (Roche, Prenzberg, Germany), 10 ng/ml epidermal growth factor, 0.4 µg/ml hydrocortisone, 0.135 mM adenine, 2 nM triiodothyronine, 0.1 nM choleratoxin, 2 mM L-glutamine (all from Sigma-Aldrich, Munich, Germany), 50 U/ml penicillin, and 50 µg/ml streptomycin in DMEM with sodium pyruvate/Ham's F12 (3:1; all from Life Technologies, Darmstadt, Germany). Outgrowth of the hair follicle-derived cells occurs within 2–3 weeks. The cells were then harvested by trypsinisation with 0.05% trypsin and 0.02% ethylenediaminetetraacetic acid and either cultivated in keratinocyte serum-free medium (K-SFM, Life Technologies, Darmstadt, Germany) to obtain hair follicle-derived keratinocytes (HFDK) or in the outgrowth medium without postmitotic 3T3-J2 fibroblasts to obtain hair follicle-derived fibroblasts (HFDF). After 4 days, HFDF were further cultivated in DMEM supplemented with 10% FBS and 2 mM L-glutamine. The cells were used at passage 3–4.

2.2 | Isolation of interfollicular primary human fibroblasts and keratinocytes

Normal human keratinocytes (NHK) and fibroblasts (NHDF) were isolated from juvenile foreskin following circumcision (age between 2 and 11 years, with ethical approval, EA1/081/13) according to standard procedures. Keratinocytes were cultivated in keratinocyte basal medium (Lonza, Basel, Switzerland) supplemented with insulin, hydrocortisone, human epidermal growth factor, and bovine pituitary extract (keratinocyte growth medium) as provided by the manufacturer. Fibroblasts were cultivated in DMEM supplemented with 10% FBS and 2 mM L-glutamine. The cells were used at passage 3–4.

2.3 | Generation of skin equivalents

Skin equivalents were generated as described previously (Hönzke et al., 2016). First, bovine collagen I (PureCol; Advanced BioMatrix, San Diego, CA, USA), FBS, and fibroblasts isolated from the hair follicles or foreskin were mixed, brought to a neutral pH, and poured into 6-well cell culture inserts (BD Biosciences, Heidelberg, Germany). After incubation at 37 °C for 2 hr, keratinocyte growth medium was added, and NHK or HFDK was seeded on top of the collagen matrix. After 24 hr, the skin equivalents were lifted to the air–liquid interface, and the medium was changed to a differentiation medium consisting of FBS (Biochrom, Berlin, Germany), 5 µg/ml insulin (Roche, Prenzberg, Germany), 10 ng/ml epidermal growth factor, 0.4 µg/ml hydrocortisone, 0.18 mM adenine, 0.1 nM choleratoxin, and 4 mM L-glutamine (all from Sigma-Aldrich, Munich, Germany) in DMEM with sodium pyruvate/Ham's F12 (Life Technologies, Darmstadt, Germany). Media changes were performed every other day. After 14 days, skin equivalents were harvested and used for further investigations.

2.4 | Histology and immunofluorescence

Skin equivalents and freshly excised human skin obtained from plastic surgeries (ethical approval, EA1/081/13) were embedded in tissue freezing medium (Leica Biosystems, Nussloch, Germany) and shock-frozen with liquid nitrogen. Subsequently, vertical sections (7 µm) were cut with a Leica CM1510 S cryotome (Leica Biosystems, Nussloch, Germany). For histological analysis by light microscopy, skin sections were stained with haematoxylin and eosin (Carl Roth, Karlsruhe, Germany) according to standard protocols.

For immunofluorescence, skin sections and primary cells were fixed with 4% formaldehyde or ice-cold methanol, washed with PBS containing 0.0025% BSA and 0.025% Tween 20 (Carl Roth, Karlsruhe, Germany), and blocked with normal goat serum (1:20 in PBS). The cells or tissue sections were then incubated with primary antibodies

overnight at 4 °C (in PBS, 0.0025% BSA, 0.025% Tween 20; Table S1). After washing, fixed sections or cells were incubated for 1 hr at room temperature with secondary antibodies IgG Alexa Fluor®488 and IgG Alexa Fluor®594 (Abcam, Cambridge, UK; 1:400 in PBS, 0.0025% BSA, 0.025% Tween 20), embedded in 4′,6-diamidin-2-phenylindol antifading mounting medium (Dianova, Hamburg, Germany) and analysed by fluorescence microscopy (BZ-8000; Keyence, Neu-Isenburg, Germany).

2.5 | Real-time quantitative polymerase chain reaction

The epidermis of skin equivalents was gently peeled from the dermis. Both parts were then milled for 30 s at 25 Hz using a TissueLyzer (Qiagen, Hilden, Germany). Subsequently, RNA was isolated using an InnuPREP RNA Mini Kit (Analytik Jena, Jena, Germany) according to the manufacturer's instructions. For cDNA synthesis, the iScript cDNA Kit (Bio-Rad, Munich, Germany) was used. Subsequently, real-time quantitative polymerase chain reaction was performed using the iTaq™ Universal SYBR® Green Supermix Kit (Bio-Rad, Munich, Germany). The primer sequences are listed in Table S2. Glyceraldehyde-3-phosphate dehydrogenase served as the housekeeping gene. Additionally, genomic DNA of hair follicle-derived fibroblasts and mouse embryonic fibroblast line 3T3-J2 were isolated using an InnuPREP DNA Mini Kit (Analytik Jena, Jena, Germany) according to the manufacturer's instructions. The genomic DNA was analysed by a Taqman chemistry-based, real-time duplex polymerase chain reaction to quantify human and murine DNA in a single-tube reaction (Nitsche et al., 2001).

2.6 | Western blot

The epidermis of skin equivalents was gently peeled off, lysed in radioimmunoprecipitation assay buffer, and the total protein concentrations determined using the Pierce® BCA Protein Assay Kit (Thermo Scientific, Waltham, USA). Subsequently, samples (~30 µg protein) were boiled in standard SDS-PAGE sample buffer and separated by 10% SDS polyacrylamide gel electrophoresis (Bio-Rad, Munich, Germany). Samples were then blotted onto nitrocellulose membranes (Bio-Rad, Munich, Germany) that were then blocked with 5% skimmed-milk powder for 1 hr at 37 °C. Subsequently, the membranes were incubated with the primary antibodies (Table S1) at 4 °C overnight and incubated with horseradish peroxidase-conjugated anti-mouse or anti-rabbit secondary antibody (Cell Signaling, Frankfurt/Main, Germany) for 1 hr. Blots were then developed with SignalFire™ ECL reagent (Cell Signaling, Frankfurt/Main, Germany) and visualised by PXi/PXi Touch Multi-Application Gel Imaging System (Syngene, Cambridge, UK). Protein expression was semiquantified by densitometry and normalised to β-actin or ß-tubulin levels using ImageJ Version 1.46r (National Institutes of Health, Bethesda, MD, USA; Schneider, Rasband, & Eliceiri, 2012).

2.7 | Ultrastructural analysis

Skin equivalents were fixed in Karnovsky solution (7.5% glutaraldehyde and 3% paraformaldehyde; all from Carl Roth, Karlsruhe, Germany), washed in 0.1 M cacodylate buffer (cacodylic acid sodium salt trihydrate; Carl Roth, Karlsruhe, Germany), and then incubated with 1% osmium tetroxide (Chempur, Karlsruhe, Germany). Dehydration was performed in an ascending series of ethanol, followed by the intermedium propylene oxide (1,2-epoxypropan; VWR, Darmstadt, Germany). Samples were embedded in a mixture of agar 100 (epoxy resin), dodecenylsuccinic anhydride (softener), methyl-5-norbornene-2,3-dicarboxylic anhydride (hardener), and 2,2-dimethoxypropane 30 (catalyst; all: Agar Scientific, Stansted, UK). Overnight, the samples polymerised at 45 and 55 °C, each for 24 hr. An ultra-microtome, Reichert Ultracut S (Leica, Wetzlar, Germany), was used to cut semi- (0.5 µm) and ultra-thin sections (80 nm). After staining the semi-thin sections with modified Richardson solution (Richardson, Jarett, & Finke, 1960) on an electric hotplate (80 °C) and examined by light microscopy (Axioskop, Carl Zeiss, Oberkochen, Germany), ultra-thin sections were mounted on nickel-grids (Agar Scientific, Stansted, UK), contrasted with 2% uranylacetate (Agar Scientific, Stansted, UK), and stabilised lead citrate (Ultrostain II, Leica, Wetzlar, Germany). Sections were then analysed by electron microscopy (Zeiss EM109, Aalen/Oberkochen, Germany).

2.8 | Skin absorption testing

Skin permeability studies were performed according to validated test procedures (OECD, 2004). Radioactively labelled testosterone served as lipophilic test compound with a total radioactivity of 2 µCi/ml. A testosterone stock solution (40 µg/ml, 2% [*v*/v] Igepal® CA-630, Sigma-Aldrich, Munich, Germany) was spiked with an appropriate amount (100 Ci/mmol) of 2,4,6,7-^{3}H-testosterone (Amersham, Freiburg, Germany). Permeation experiments were performed using Franz diffusion cells (PermeGear, Hellertown, PA, USA), where 500 µl of the receptor fluid was sampled every 30 min for 6 hr. The total amount of permeated testosterone was quantified using radiochemical detection (HIDEX 300 SL, HIDEX, Turku, Finland). The permeation rate of testosterone was calculated as the apparent permeability coefficient (P_{app}).

2.9 | Statistical analysis

The unpaired student's *t*-test was used for direct comparisons of two independent groups using SigmaPlot 11.0 (Systat Software GmbH, Erkrath, D). Asterisks (*) indicate statistical significance over skin equivalents grown from skin-derived cells, and $p \leq 0.05$ was considered statistical significant. Data from at least three independent experiments are presented as means ± standard error of the mean (SEM).

3 | RESULTS

3.1 | Keratinocytes and fibroblasts derived from hair follicles or skin do not show any significant differences in cell-specific markers

HFDF and HFDK were characterised and compared with their interfollicular counterparts, respectively, NHDF and NHK. No differences in the expression of the fibroblast-specific markers vimentin

and desmin were seen. The number of cells expressing alpha-smooth muscle actin and versican was slightly higher in hair follicle-derived fibroblasts (Figure 1a). Similarly, no perceivable differences were detected between primary cultures of HFDKs and NHKs. Keratinocytes from both sources were positive for CK5, CK14, and CK17, markers characteristic of mitotically active basal cells. Differentiation-specific CK10 was not expressed in either HFDK or NHK.

HFDF were negative for the keratinocyte-specific CK14, clearly differentiating them from HFDK (data not shown). Additionally, HFDF, NHDF, HDFK, and NHK were analysed for the expression of type I collagen *(COL1A1)* and type IV collagen *(COL4A1)*, alpha-smooth muscle actin *(ACTA2)*, interleukin-1 alpha *(IL1A)*, -6 *(IL6)* and -8 *(IL8)*, and transforming growth factor-beta *(TGFB)* at the mRNA level (Figure S2). Again, comparable gene expression profiles were observed.

To distinguish HFDF from the mouse embryonic fibroblast line 3T3-J2, which served as feeder cells during the cell outgrowth, genomic DNA of both cell types was analysed using real-time duplex polymerase chain reaction. No murine DNA was detected in hair follicle-derived fibroblasts (Figure S3).

3.2 | Skin equivalents generated from hair follicle-derived cells show slightlyless well organised epidermal layers but comparable epidermal differentiation and proliferation

Skin equivalents were generated using the following cell combinations: NHK and NHDF, NHK and HFDF, HFDK and NHDF, and HFDK and HFDF. Analysis by light-microscopy revealed the development of all epidermal layers (Figures 2a and S4). Some histological differences between the cell combinations were observed with regard to cell shapes and organisation of strata. In the skin equivalents generated from HFDKs, the cells of the epidermal layers appeared more irregularly shaped compared with those of skin equivalents generated from NHKs. Additionally, spheroid structures located within the supra-basal layers were found exclusively in skin equivalents generated from HFDK. For all skin equivalents, the viable epidermis stained positively for CK10 in suprabasal cell layers and CK14 throughout the epidermis (Figure 2b), the latter of which differs from the distribution seen in native human skin, perhaps due to the culture conditions (Figure S5A). No significant differences in cell proliferation

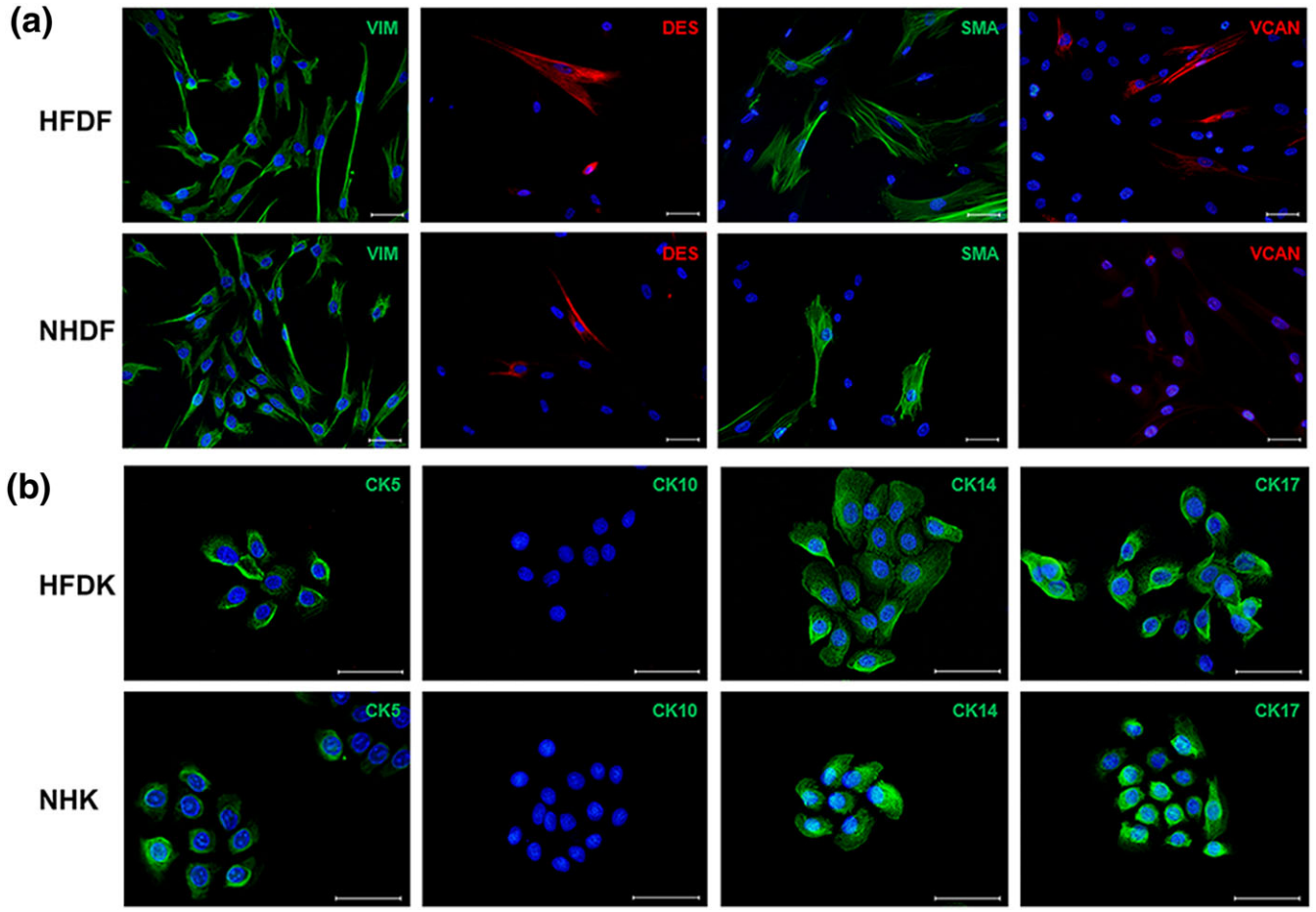

FIGURE 1 Immunostaining of fibroblast- and keratinocyte-specific markers. (a) Representative immunostaining of fibroblasts derived from hair follicle (hair follicle-derived fibroblast [HFDF]) and skin (normal human dermal fibroblast [NHDF]) for vimentin (VIM, green), desmin (DES, red), alpha-smooth muscle actin (SMA, green), and versican (VCAN, red). (b) Representative immunostaining of keratinocytes isolated from hair follicles (hair follicle-derived keratinocyte [HFDK]) and skin (normal human keratinocyte [NHK]) for the cytokeratins (CK)5, CK10, CK14, and CK17. Counterstaining was performed with 4′,6′-diamin-2-phenylindol (blue). Scale bar = 50 μm. $n = 4$

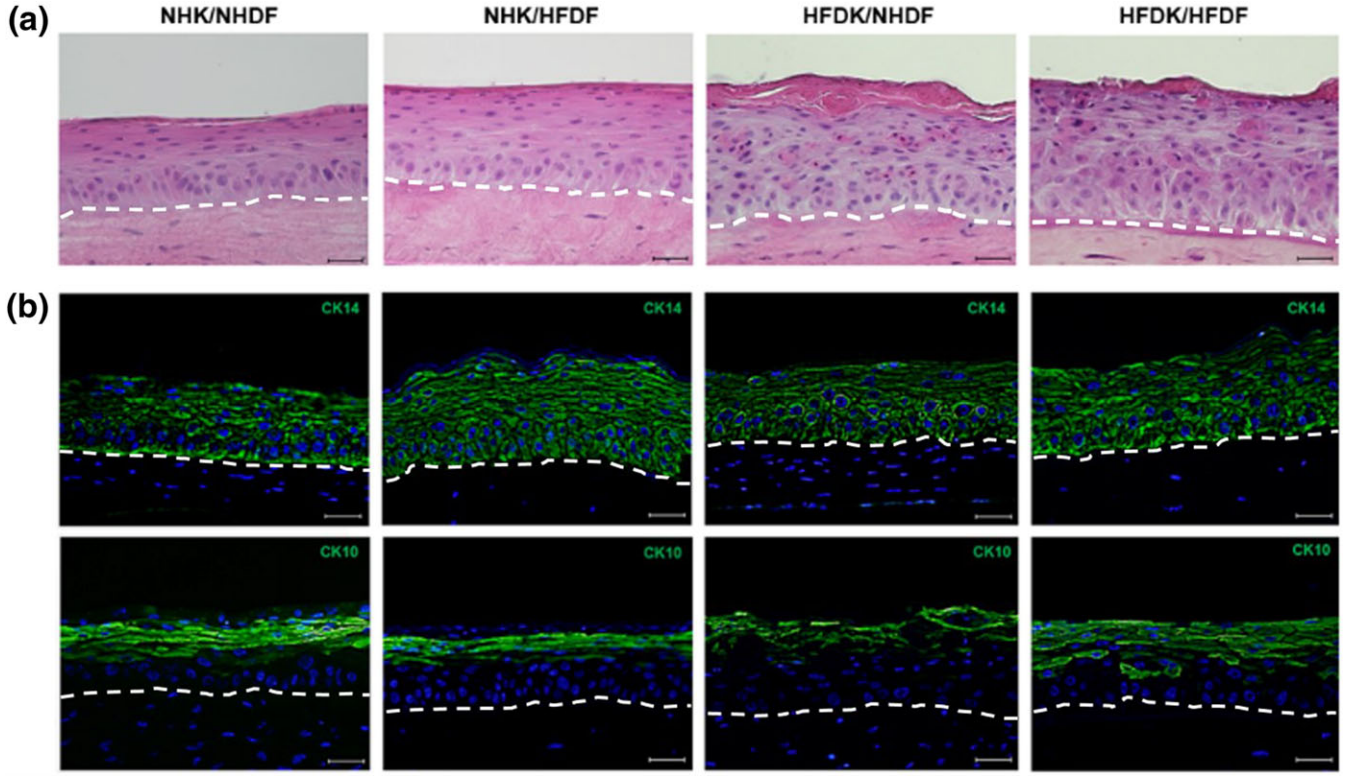

FIGURE 2 Histological analysis of skin equivalents generated from interfollicular and hair follicle-derived cells. (a) Representative haematoxylin and eosin staining of the skin equivalents grown from interfollicular (normal human dermal fibroblast [NHDF] and normal human keratinocyte [NHK]) or hair follicle-derived keratinocytes (HFDK) and/or fibroblasts (HFDF). (b) Representative immunostaining against the basal cell marker CK14 (green, top row) and terminal differentiation marker CK10 (green, bottom row) of the skin equivalents. Counterstaining of cell nuclei was performed with 4′,6′-diamin-2-phenylindol (blue). Scale bar = 100 μm. n = 3

were observed between any of the skin equivalents and native human skin as assessed by Ki67 staining (Figure S6).

3.3 | Skin equivalents grown from hair follicle-derived cells show reduced intercellular space in the stratum basale and improved sub-basal layer histology

Analysis of semi- and ultra-thin sections by electron microscopy confirmed the expression of all strata in the skin equivalents (Figure S4), distinguishable by characteristic morphological and ultrastructural features. The stratum basale was characterised as the layer in which cells come into direct contact with the dermal equivalent. The stratum spinosum was defined as the supra basal layer of cells with typical spinous processes. The stratum granulosum was determined by the presence of electron-dense intracellular granula, and the superficial stratum corneum was defined as layer populated by corneocytes that are absent of organelles or nuclei.

Interestingly, skin equivalents comprising either NHK and NHDF or NHK and HFDF showed greater similarity to one another than skin equivalents generated from HFDK (Figure S4). The basal cells of skin equivalents generated from the latter were irregularly shaped: columnar, polygonal, and elongated cells were present that made it difficult to distinguish the basal layer from adjacent supra basal layers. In addition, individual supra basal cells lacked spinous processes and spheroidal structures composed of either cells (up to nine cells, including mitotic cells) or cell remnants and amorphous material that were integrated into the supra basal layers (Figure 3b).

Interestingly, in skin equivalents grown from HFDKs, neighbouring basal cells and individual supra basal cells adhered tightly to each other by interdigitating protrusions not seen in any other skin equivalent (Figure 3aI). Furthermore, at the dermal-epidermal interface, a sub-basal layer of extracellular material resembling a basal lamina was detected. Puncta of electron-dense membrane plaques that anchored to the sub-basal extracellular material were observed at the basal poles of the basal cells. Interestingly, although both the sub-basal layer and the membrane plaques were distinct and regularly seen in skin equivalents grown from hair follicle-derived cells, they were rarely observed in skin equivalents generated from interfollicular cells (Figure 3aI–IV). Nonetheless, NHK/NHDF and NHK/HFDF skin equivalents clearly displayed more regular formed basale and spinosal layers (Figures 2 and S4). The cells of the stratum basale were mainly columnar (70%), but in contrast to the HFDK equivalents, intercellular spaces were observed between the basal cells (Figure 3aI). The spinous cells were ellipsoid in shape within the deeper layers, whereas those of the upper layers appeared flattened (Figure 3bI).

In all types of constructs, the cells of the stratum granulosum were flattened and densely packed and populated by lamellar bodies and keratohyaline granules (Figure 3c). The stratum corneum was characterised by enucleated, flattened cells surrounded by a well developed cornified envelope. In the NHK/NHDF and NHK/HFDF skin equivalents, the cornified cell layers were regularly and tightly

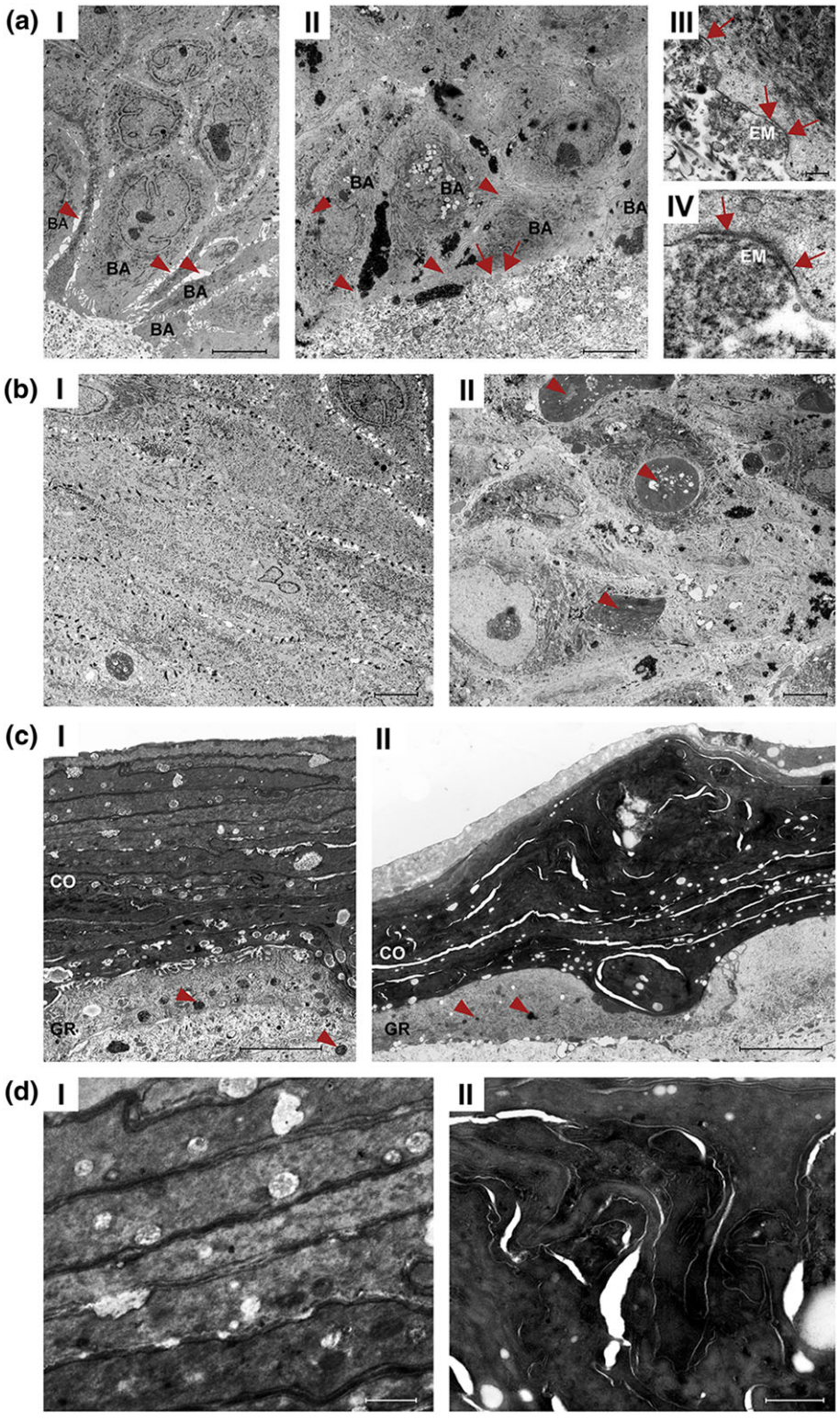

FIGURE 3 Transmission electron microscopy images of a skin-derived (I) and a hair follicle-derived skin equivalent (II, III, and IV). In (aI), the cells of the basal layer (BA) are columnar (arrowheads; wide intercellular spaces). (aII) Columnar, polygonal, and elongated cells of the BA tightly adhered to one another (arrowheads; (P) electron-dense particles). Scale bar = 5,000 nm. (aIII, IV) Magnifications of (aII), cell membrane plaques (arrows) and sub-basal layer of extracellular material (EM). Scale bar III = 500 nm, scale bar IV = 250 nm. (bI) Spinous cells are regularly organised and of an ellipsoid shape. (bII) Cuboidal or irregularly shaped spinous cells; amorphous material forming spheroidal structures (arrowheads). (cI, II) Keratohyaline granule (arrowhead) in upper layers of the stratum granulosum (GR); stratum corneum (CO) with enucleated, flattened corneocytes, tightly packed with highly organised keratin filaments. Scale bar = 5,000 nm. (dI) Regularly and tightly packed corneocytes. (dII) Cornified cell layers folded and intertwined into each other; gaps between corneocytes. Scale bar = 1,000 nm. *n* = 3

packed with corneocytes that adhered to each other through corneodesmosomes (Figure 3dI). By contrast, the HFDK skin equivalents showed cornified cell layers of varied architecture; in addition to longitudinal arrangements, corneocytes were also found folded and intertwined into each other or with gaps between them (Figure 3dII).

3.4 | Skin equivalents grown from hair follicle-derived cells show altered expression levels of skin barrier and tight junction proteins

The structural proteins involucrin, filaggrin, and loricrin were expressed in all skin equivalents (Figure 4). Interestingly, filaggrin expression was significantly reduced, and involucrin expression significantly increased, in skin equivalents grown from HFDK and HFDF as compared with skin equivalents generated using interfollicular cells (NHK/NHDF; Figure 4a). No major differences were observed in the expression profile of loricrin (Figure 4b). Compared with human skin, all skin equivalents expressed less filaggrin but comparable levels of involucrin and loricrin (Figure S5B).

Similar to the skin barrier proteins, the expression of the tight junction proteins claudin 1 and occludin differed between skin equivalents generated from interfollicluar or hair follicle-derived cells (Figure 5a). Occludin expression was lower in the skin equivalents grown from hair follicle-derived cells compared with interfollicular cells. Significantly, greater levels of claudin 1 expression were seen in skin equivalents grown from HFDK and HFDF (Figure 5b). Overall, the expression pattern of claudin 1 was comparable with human skin (Figure S5C) for all skin equivalents. By contrast, occludin expression is mostly observed in the upper strata of human skin and does not appear in the whole epidermis as it did in all the generated skin equivalents (Figure S5C). Corresponding mRNA expression levels are depicted in Figure S7.

3.5 | Skin equivalents generated from hair follicle-derived keratinocytes showed increased expression of types IV and VII collagen

Immunostaining against the basement membrane proteins types IV and VII collagen and laminin 5 confirmed their expression in all skin equivalents (Figure 6). Notably, the highest expressions of types IV and VII collagen were observed in skin equivalents generated from hair follicle-derived keratinocytes. Laminin 5 was detected in the epidermal–dermal junction as a linear stain with similar expression levels in all skin equivalents. Notably, skin equivalents grown from hair follicle-derived keratinocytes showed great similarities to human skin with regard to the basement membrane proteins (Figures 6 and S5D). Corresponding mRNA expression levels were also seen (Figure S8).

3.6 | Skin equivalents grown from hair follicle-derived cells show similar skin barrier function

The barrier functions of skin equivalents grown from interfollicular or hair follicle-derived cells were assessed by permeation studies, where no significant differences were found (Figure S9). However, though non-significant, a trend towards increased skin permeability was observed for skin equivalents generated from hair follicle-derived cells. These showed an apparent permeability (P_{app}) value of $9.6^{-6} \pm 6.8^{-7}$ (cm/s) as compared with a P_{app} value of $7.8^{-6} \pm 8.2^{-7}$ (cm/s) for skin equivalents formed of skin-derived keratinocytes and fibroblasts.

4 | DISCUSSION

Over the past 10 years, great efforts have been made to generate organotypic models of the human skin for applications ranging from regenerative medicine to alternatives to animal testings. To date, several protocols have been established, describing the cultivation of skin equivalents using cell lines, primary skin-derived keratinocytes and fibroblasts, and addition of further cell types such as melanocytes, immune cells, or stem cells (Asbill et al., 2000; Duval et al., 2012; Laco, Kun, Weber, Ramakrishna, & Chan, 2009; Ouwehand et al., 2011; Reijnders et al., 2015; Thakoersing et al., 2012). Approaches using patient-derived cells for the generation of skin equivalents have almost exclusively relied on skin biopsies, a method associated with impaired wound healing, scar formation, and infections (Nischal, Nischal, & Khopkar, 2008). Although keratinocytes can be obtained from plucked hair follicles, the isolation of fibroblasts was only possible using microdissections of the human scalp, which again is an invasive procedure (Driskell, Clavel, Rendl, & Watt, 2011; Gledhill, Gardner, & Jahoda, 2013; Higgins et al., 2017).

Hence, we aimed to develop a non-invasive protocol enabling the isolation of primary keratinocytes and fibroblasts from plucked scalp hair follicles. For this purpose, outgrown hair follicle-derived cells were cultured in serum-enriched cell culture medium without feeder cells for 4 days, followed by culture in a fibroblast-specific medium. As described previously, keratinocytes were obtained by cultivating hair follicle-derived cells either directly in keratinocyte-specific culture medium or with feeder cells in specific serum-enriched culture medium (Aasen & Izpisua Belmonte, 2010; Limat & Hunziker, 2002). To ensure the comparability of these to interfollicular keratinocytes and fibroblasts, thorough characterisations of both were performed. For fibroblasts, we analysed the expression of vimentin, desmin, alpha-smooth muscle actin, and versican. These markers are more or less fibroblast-specific; a true characteristic marker of skin fibroblasts has not yet been described (Kalluri & Zeisberg, 2006). Vimentin, for example, is expressed in all fibroblast types but is also detectable on endothelial cells (Mork, van Deurs, & Petersen, 1990). Similarly, desmin is expressed in smooth muscle cells in addition to skin fibroblasts (Schmid et al., 1982). Overall, no differences in the expression between interfollicular (NHDF) and HFDF were observed except for slightly higher alpha-smooth muscle actin and versican levels in HFDFs, likely because these are also markers for the dermal sheath and dermal papilla (Jahoda, Reynolds, Chaponnier, Forester, & Gabbiani, 1991; Yang & Cotsarelis, 2010) and should only be expressed to a low extent in normal skin fibroblasts (Gabbiani, 2003; Gabbiani, Ryan, & Majne, 1971).

Interestingly, the origin of our isolated HFDFs is presently indeterminable. Plucking hair follicles excludes the extraction of the dermal

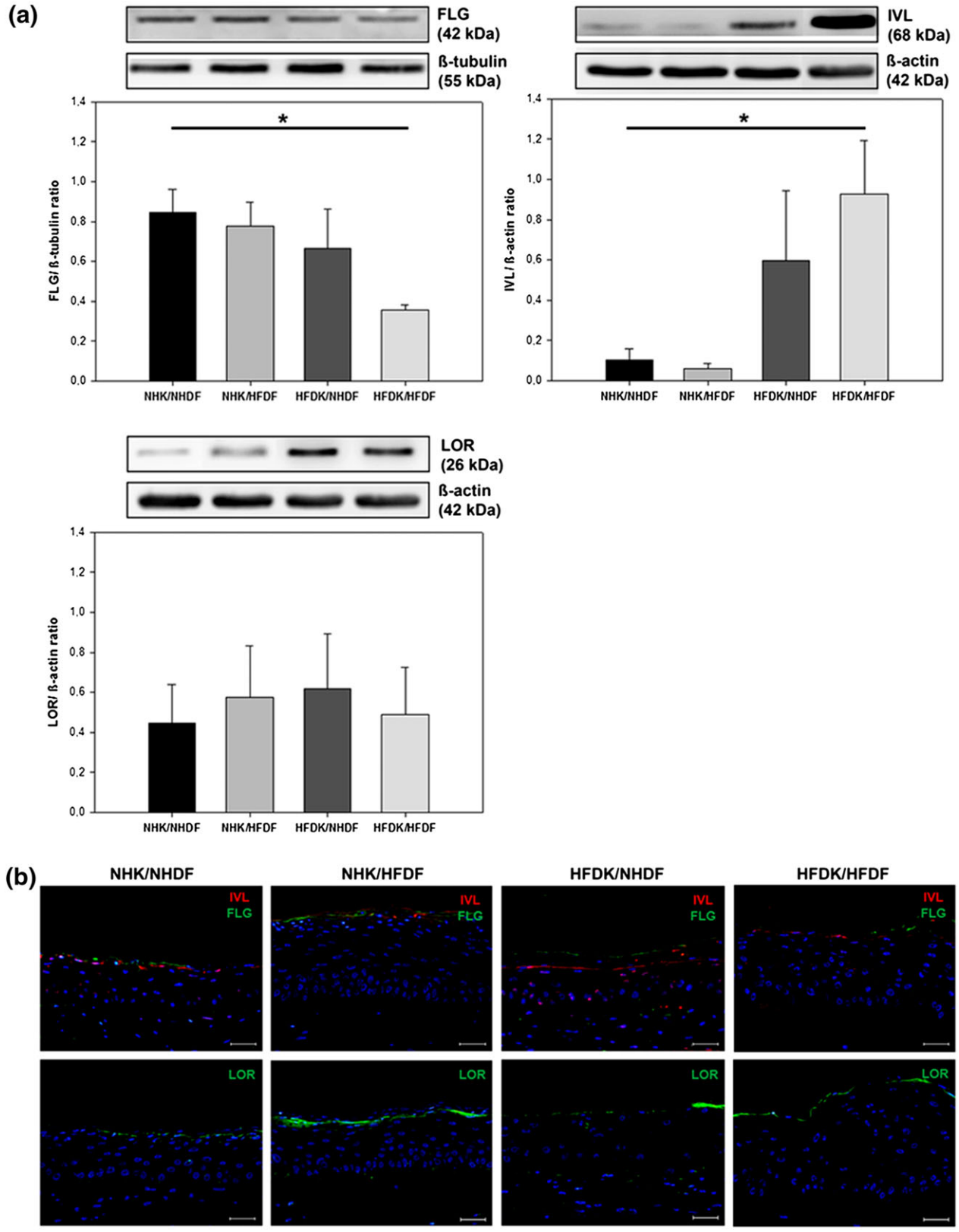

FIGURE 4 Expression profiles of the skin differentiation markers involucrin (IVL), filaggrin (FLG), and loricrin (LOR) in skin equivalents generated from interfollicular and hair follicle-derived keratinocytes and fibroblasts. (a) Western blots and relative protein expression semiquantified by densitometry of skin equivalents generated from interfollicular (normal human keratinocyte [NHK] and normal human dermal fibroblast [NHDF]) and hair follicle-derived keratinocytes [HFDK] and hair follicle-derived fibroblasts [HFDF]). (b) Representative immunostaining in the skin equivalents against FLG (green), IVL (red) and LOR (green). Counterstaining of cell nuclei was performed with 4′,6′-diamin-2-phenylindol (blue). Scale bar = 100 µm. Values are given as mean ± SEM. $n = 3$. * indicates statistically significant differences from skin equivalents generated from interfollicular keratinocytes and fibroblasts (NHK/NHDF; $^*p \leq 0.05$)

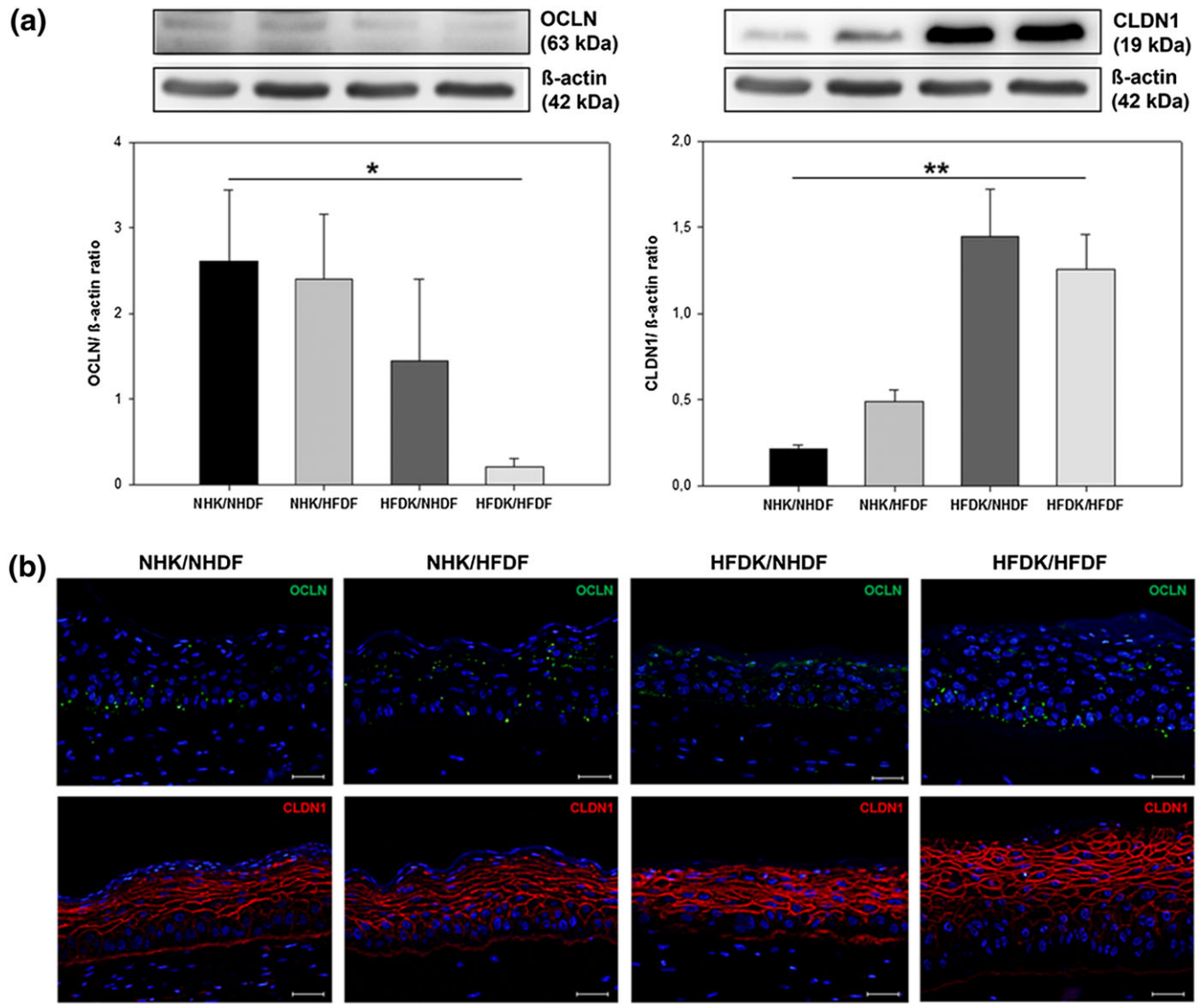

FIGURE 5 Expression profiles of the tight junction proteins occludin (OCLN) and claudin 1 (CLDN1) in skin equivalents grown from interfollicular (normal human keratinocyte [NHK] and normal human dermal fibroblast [NHDF]) or hair follicle-derived keratinocytes (HFDK) and fibroblasts (HFDF). (a) Western blots and relative protein expression semiquantified by densitometry. (b) Representative immunostaining against the tight junction proteins OCLN (green) and CLDN1 (red). Counterstaining of cell nuclei was performed with 4′,6′-diamin-2-phenylindol (blue). Scale bar = 100 μm. Values are given as mean ± SEM. $n = 3$. * indicates statistically significant differences from NHK/NHDF skin equivalents (*$p \leq 0.05$, **$p \leq 0.01$)

papilla in most cases, a known location of mesenchymal cells (Bassukas & Hornstein, 1989; Rompolas & Greco, 2014). Dermal sheath cells are the other known population of fibroblasts in the hair follicle, the isolation of which was previously only possible following microdissections (Higgins et al., 2017; McElwee & Sinclair, 2008; Yang & Cotsarelis, 2010). Interestingly, the initial outgrowth of the ORS cells reported here showed spindle-shaped cells at their edge (Figure S1B) potentially indicating an origin from the dermal sheath. Importantly, it was verified that the isolated fibroblasts are human and not residues from the murine feeder cells (Figure S3).

To ensure a successful outgrowth of hair follicle-derived cells and a high cell yield, proper contact between the hairs and the culture dish is essential (Aasen & Izpisua Belmonte, 2010). Both HFDKs and HFDFs were cultured to passage 3–4, which is comparable with interfollicular cells. Nevertheless, it has to be noted that less keratinocytes (~0.9 to 2.5 million cells in p0) can be obtained from plucked hair follicles compared with skin biopsies.

Following successful isolation of cells from plucked hair follicles, we cultivated skin equivalents from these and compared them to skin equivalents grown from interfollicular keratinocytes and fibroblasts. Histological analyses showed comparable differentiation and proliferation of all skin equivalents (Figures 2, S4, and S6), although a less well organised epidermis in skin equivalents generated from hair follicle-derived cells was observed. Concordantly, ultrastructural analysis showed few but distinct differences between interfollicular and hair follicle-derived skin equivalents. For example, spheroidal structures containing cellular or noncellular debris were exclusively found in skin equivalents grown from hair follicle-derived keratinocytes (Figure 2a). These may be an artefact of early keratinisation of the ORS cells and constitute apoptotic cells or due to contaminating epidermal stem

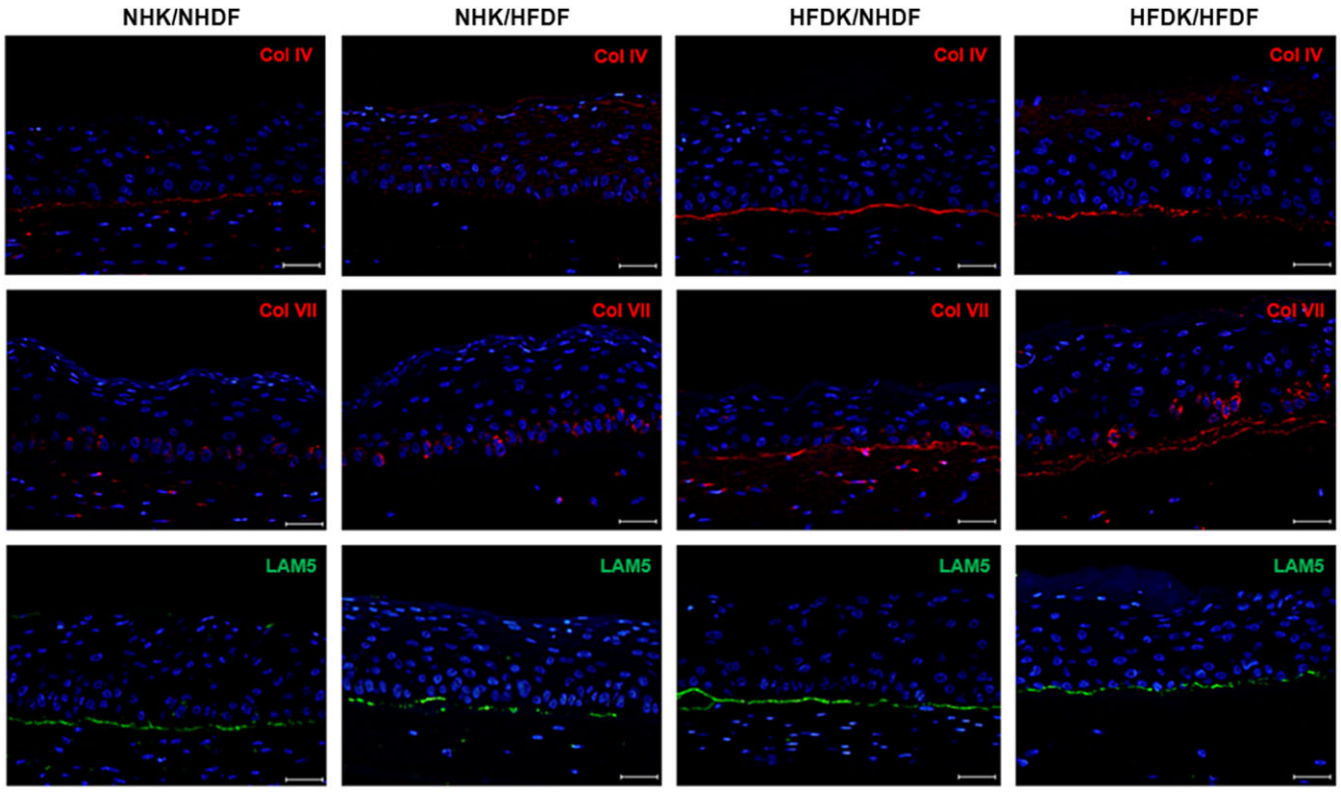

FIGURE 6 Expression of the basement membrane proteins types IV and VII collagen and laminin 5 in skin equivalents grown from interfollicular or hair follicle-derived keratinocytes (HFDK) and fibroblasts (HFDF). Representative immunostaining against the basement membrane proteins type IV collagen (Col IV, red), type VII collagen (Col VII, red), and laminin 5 (LAM5, green). Counterstaining of cell nuclei was performed with 4′,6′-diamin-2-phenylindol (blue). Scale bar = 100 μm. *n* = 3. NHK = normal human epithelial keratinocyte; NHDF = normal human dermal fibroblast

cells, which tend to organise in clusters and adhere to each other by a multitude of adhesion proteins. Alternatively, the speroids may be apoptotic remnants of epidermal stem cell clusters that did not receive adequate developmental cues to undergo further processing (Rzepka, Schaarschmidt, Nagler, & Wohlrab, 2005). In line with this, differences in the clonogenic potential of cells from different regions of microdissected mouse hair follicles were previously demonstrated (Claudinot, Nicolas, Oshima, Rochat, & Barrandon, 2005), another potential explanation for these structures.

Interestingly, the formation of electron-dense extracellular sub-basal material appeared improved in hair follicle-derived skin equivalents indicating the development of a basal lamina (Figure 3). Increased expression of types IV and VII collagen further supports this finding (Figure 6). In addition, puncta of electron-dense membrane plaques were found in the hair follicle skin equivalents anchored to the sub-basal electron-dense material, potentially indicating the formation of hemidesmosomes. This might be attributed to improved communication between keratinocytes and fibroblasts derived from the hair follicle of the same donor. These findings are in line with recent work showing a positive influence of dermal papilla and sheath cells on basal lamina formation (Higgins et al., 2017) when hair follicle-derived keratinocytes and fibroblasts from the same donor were used.

Although all skin equivalents expressed all expected epidermal layers, cell shape and organisation of the strata differed from native human skin (Figure S5). Differences were also observed in the expression patterns of filaggrin and involucrin (Figure 4), as well as the tight junction proteins claudin 1 and occludin (Figure 5). Whether this is due to inter-individual differences or to the different cell origins is unclear. Although no statistically significant differences were found between the skin barrier function any of the skin equivalents (Figure S9), a slight trend towards increased skin permeability was seen for the skin equivalents grown from hair follicle-derived cells. This may be due to their less well organised epidermal layers as compared with skin equivalents grown from interfollicular cells (Figure 2). Potential reasons for this include the different cell origins (scalp *vs*. foreskin) and the donors' age (20–30 *vs*. ≤8 years). However, in our experience, age does not cause a major impact because cells from older donors mainly show decreased proliferation rates rather than reduced abilities to form stratified tissues.

In summary, we have successfully established a method to isolate fibroblasts from plucked hair follicles without invasive procedure. Moreover, though differences between skin equivalents generated from keratinocytes and fibroblasts originating from hair follicles and interfollicular regions were observed, these were relatively minor especially in terms of epidermal stratification.

This method could be of particular use for the generation of skin disease models because it allows the isolation of patient-derived cells from plucked hair follicles without invasive procedures. This is of specific interest for skin disorders with a genetic background such as atopic dermatitis, psoriasis, or autosomal recessive congenital ichthyoses.

ACKNOWLEDGEMENT

Financial support by the Berlin-Brandenburg research platform BB3R is gratefully acknowledged (S. H. and A. L.). The authors wish to thank Franziska Ermisch and Verena Holle from the Institute of Veterinary Anatomy, Department of Veterinary Medicine for their consistent excellent technical support. Thanks to Dr. Guy Yealland for language editing.

CONFLICT OF INTEREST

The authors declare no competing financial interests.

AUTHOR CONTRIBUTIONS

A. L. and S. K. performed the experiments. S. H. supervised the work. A. L., S. K., A. V., and S. H. designed the experiments, analysed data, and wrote the manuscript. All authors provided critical review of the manuscript.

ORCID

Sarah Hedtrich http://orcid.org/0000-0001-6770-3657

REFERENCES

Aasen, T., & Izpisua Belmonte, J. C. (2010). Isolation and cultivation of human keratinocytes from skin or plucked hair for the generation of induced pluripotent stem cells. *Nature Protocols*, *5*(2), 371–382. https://doi.org/10.1038/nprot.2009.241

Amelian, A., Wasilewska, K., Megias, D., & Winnicka, K. (2017). Application of standard cell cultures and 3D in vitro tissue models as an effective tool in drug design and development. *Pharmacological Reports*, *69*(5), 861–870. https://doi.org/10.1016/j.pharep.2017.03.014

Asbill, C., Kim, N., El-Kattan, A., Creek, K., Wertz, P., & Michniak, B. (2000). Evaluation of a human bio-engineered skin equivalent for drug permeation studies. *Pharmaceutical Research*, *17*(9), 1092–1097.

Bassukas, I. D., & Hornstein, O. P. (1989). Effects of plucking on the anatomy of the anagen hair bulb. A light microscopic study. *Archives of Dermatological Research*, *281*(3), 188–192.

Cho, H. J., Bae, I. H., Kim, D. S., Im Na, J., & Park, K. C. (2004). The reconstruction of skin equivalents with hair follicle dermal sheath cells. 조직공학과 재생의학, *1*(2), 143–148.

Claudinot, S., Nicolas, M., Oshima, H., Rochat, A., & Barrandon, Y. (2005). Long-term renewal of hair follicles from clonogenic multipotent stem cells. *Proceedings of the National Academy of Sciences of the United States of America*, *102*(41), 14677–14682. https://doi.org/10.1073/pnas.0507250102

Driskell, R. R., Clavel, C., Rendl, M., & Watt, F. M. (2011). Hair follicle dermal papilla cells at a glance. *Journal of Cell Science*, *124*(Pt 8), 1179–1182. https://doi.org/10.1242/jcs.082446

Duval, C., Chagnoleau, C., Pouradier, F., Sextius, P., Condom, E., & Bernerd, F. (2012). Human skin model containing melanocytes: Essential role of keratinocyte growth factor for constitutive pigmentation-functional response to alpha-melanocyte stimulating hormone and forskolin. *Tissue Engineering. Part C, Methods*, *18*(12), 947–957. https://doi.org/10.1089/ten.TEC.2011.0676

Gabbiani, G. (2003). The myofibroblast in wound healing and fibrocontractive diseases. *The Journal of Pathology*, *200*(4), 500–503. https://doi.org/10.1002/path.1427

Gabbiani, G., Ryan, G. B., & Majne, G. (1971). Presence of modified fibroblasts in granulation tissue and their possible role in wound contraction. *Experientia*, *27*(5), 549–550.

Gho, C., Braun, J., Tilli, C., Neumann, H., & Ramaekers, F. (2004). Human follicular stem cells: Their presence in plucked hair and follicular cell culture. *British Journal of Dermatology*, *150*(5), 860–868.

Gledhill, K., Gardner, A., & Jahoda, C. A. (2013). Isolation and establishment of hair follicle dermal papilla cell cultures. *Methods in Molecular Biology*, *989*, 285–292. https://doi.org/10.1007/978-1-62703-330-5_22

Guiraud, B., Hernandez-Pigeon, H., Ceruti, I., Mas, S., Palvadeau, Y., Saint-Martory, C., & Bessou-Touya, S. (2014). Characterization of a human epidermis model reconstructed from hair follicle keratinocytes and comparison with two commercially models and native skin. *International Journal of Cosmetic Science*, *36*(5), 485–493. https://doi.org/10.1111/ics.12150

Higgins, C. A., Roger, M. F., Hill, R. P., Ali-Khan, A. S., Garlick, J. A., Christiano, A. M., & Jahoda, C. A. B. (2017). Multifaceted role of hair follicle dermal cells in bioengineered skins. *The British Journal of Dermatology*, *176*(5), 1259–1269. https://doi.org/10.1111/bjd.15087

Hönzke, S., Wallmeyer, L., Ostrowski, A., Radbruch, M., Mundhenk, L., Schäfer-Korting, M., & Hedtrich, S. (2016). Influence of Th2 cytokines on the cornified envelope, tight junction proteins, and β-defensins in filaggrin-deficient skin equivalents. *The Journal of Investigative Dermatology*, *136*(3), 631–639. https://doi.org/10.1016/j.jid.2015.11.007

Jahoda, C. A., Reynolds, A. J., Chaponnier, C., Forester, J. C., & Gabbiani, G. (1991). Smooth muscle alpha-actin is a marker for hair follicle dermis in vivo and in vitro. *Journal of Cell Science*, *99*, 627–636.

Kalluri, R., & Zeisberg, M. (2006). Fibroblasts in cancer. *Nature Reviews. Cancer*, *6*(5), 392–401.

Laco, F., Kun, M., Weber, H. J., Ramakrishna, S., & Chan, C. K. (2009). The dose effect of human bone marrow-derived mesenchymal stem cells on epidermal development in organotypic co-culture. *Journal of Dermatological Science*, *55*(3), 150–160. https://doi.org/10.1016/j.jdermsci.2009.05.009

Leist, M., & Hartung, T. (2013). Inflammatory findings on species extrapolations: Humans are definitely no 70-kg mice. *Archives of Toxicology*, *87*(4), 563–567. https://doi.org/10.1007/s00204-013-1038-0

Lenoir, M. C., Bernard, B. A., Pautrat, G., Darmon, M., & Shroot, B. (1988). Outer root sheath cells of human hair follicle are able to regenerate a fully differentiated epidermis in vitro. *Developmental Biology*, *130*(2), 610–620.

Limat, A., Breitkreutz, D., Hunziker, T., Boillat, C., Wiesmann, U., Klein, E., & Fusenig, N. E. (1991). Restoration of the epidermal phenotype by follicular outer root sheath cells in recombinant culture with dermal fibroblasts. *Experimental Cell Research*, *194*(2), 218–227.

Limat, A., & Hunziker, T. (2002). Use of epidermal equivalents generated from follicular outer root sheath cells in vitro and for autologous grafting of chronic wounds. *Cells Tissues Organs*, *172*(2), 79–85. 65615

Limat, A., Hunziker, T., Boillat, C., Bayreuther, K., & Noser, F. (1989). Postmitotic human dermal fibroblasts efficiently support the growth of human follicular keratinocytes. *The Journal of Investigative Dermatology*, *92*(5), 758–762.

Limat, A., & Noser, F. K. (1986). Serial cultivation of single keratinocytes from the outer root sheath of human scalp hair follicles. *The Journal of Investigative Dermatology*, *87*(4), 485–488.

McElwee, K. J., & Sinclair, R. (2008). Hair physiology and its disorders. *Drug Discovery Today: Disease Mechanisms*, *5*(2), 163–171. https://doi.org/10.1016/j.ddmec.2008.04.001

Mistriotis, P., & Andreadis, S. T. (2013). Hair follicle: A novel source of multipotent stem cells for tissue engineering and regenerative medicine. *Tissue Engineering. Part B, Reviews*, *19*(4), 265–278. https://doi.org/10.1089/ten.TEB.2012.0422

Mork, C., van Deurs, B., & Petersen, O. W. (1990). Regulation of vimentin expression in cultured human mammary epithelial cells. *Differentiation*, *43*(2), 146–156.

Nakano, M., Kamada, N., Suehiro, K., Oikawa, A., Shibata, C., Nakamura, Y., & Ohara, O. (2016). Establishment of a new three-dimensional human epidermal model reconstructed from plucked hair follicle-derived

keratinocytes. *Experimental Dermatology*, *25*(11), 903–906. https://doi.org/10.1111/exd.13066

Nischal, U., Nischal, K., & Khopkar, U. (2008). Techniques of skin biopsy and practical considerations. *Journal of Cutaneous and Aesthetic Surgery*, *1*(2), 107–111. https://doi.org/10.4103/0974-2077.44174

Nitsche, A., Becker, M., Junghahn, I., Aumann, J., Landt, O., Fichtner, I., & Siegert, W. (2001). Quantification of human cells in NOD/SCID mice by duplex real-time polymerase-chain reaction. *Haematologica*, *86*(7), 693–699.

OECD. (2004). Guidance document no. 28 for the conduct of skin absorption studies. OECD Enviromental Health and Safety Publications Series on Testing and Assessment.

OECD (2016). *Test no. 431: In vitro skin corrosion: Reconstructed human epidermis (RHE) test method*. Paris: OECD Publishing.

Ouwehand, K., Spiekstra, S. W., Waaijman, T., Scheper, R. J., de Gruijl, T. D., & Gibbs, S. (2011). Technical advance: Langerhans cells derived from a human cell line in a full-thickness skin equivalent undergo allergen-induced maturation and migration. *Journal of Leukocyte Biology*, *90*(5), 1027–1033. https://doi.org/10.1189/jlb.0610374

Paus, R., & Cotsarelis, G. (1999). The biology of hair follicles. *The New England Journal of Medicine*, *341*(7), 491–497.

Perrin, S. (2014). Preclinical research: Make mouse studies work. *Nature*, *507*(7493), 423–425. https://doi.org/10.1038/507423a

Ramata-Stunda, A., Boroduskis, M., Vorobjeva, V., & Ancans, J. (2013). Cell and tissue culture-based in vitro test systems for evaluation of natural skin care product ingredients. *Environmental and Experimental Biology*, (11-P), 159–177.

Reijnders, C. M., van Lier, A., Roffel, S., Kramer, D., Scheper, R. J., & Gibbs, S. (2015). Development of a full-thickness human skin equivalent in vitro model derived from TERT-immortalized keratinocytes and fibroblasts. *Tissue Engineering. Part A*, *21*(17–18), 2448–2459. https://doi.org/10.1089/ten.TEA.2015.0139

Richardson, K. C., Jarett, L., & Finke, E. H. (1960). Embedding in epoxy resins for ultrathin sectioning in electron microscopy. *Stain Technology*, *35*, 313–323.

Rompolas, P., & Greco, V. (2014). Stem cell dynamics in the hair follicle niche. *Seminars in Cell & Developmental Biology*, *25–26*, 34–42. https://doi.org/10.1016/j.semcdb.2013.12.005

Rzepka, K., Schaarschmidt, G., Nagler, M., & Wohlrab, J. (2005). Epidermal stem cells. *Journal der Deutschen Dermatologischen Gesellschaft*, *3*(12), 962–973. https://doi.org/10.1111/j.1610-0387.2005.05071.x

Schembri, K., Scerri, C., & Ayers, D. (2013). Plucked human hair shafts and biomolecular medical research. *ScientificWorldJournal*, *2013*, 620531. https://doi.org/10.1155/2013/620531

Schmid, E., Osborn, M., Rungger-Brandle, E., Gabbiani, G., Weber, K., & Franke, W. W. (1982). Distribution of vimentin and desmin filaments in smooth muscle tissue of mammalian and avian aorta. *Experimental Cell Research*, *137*(2), 329–340.

Schneider, C. A., Rasband, W. S., & Eliceiri, K. W. (2012). NIH Image to ImageJ: 25 years of image analysis. *Nature Methods*, *9*(7), 671–675.

Seok, J., Warren, H. S., Cuenca, A. G., Mindrinos, M. N., Baker, H. V., Xu, W., … Tompkins, R. G. (2013). Genomic responses in mouse models poorly mimic human inflammatory diseases. *Proceedings of the National Academy of Sciences of the United States of America*, *110*(9), 3507–3512. https://doi.org/10.1073/pnas.1222878110

van Smeden, J., Janssens, M., Gooris, G. S., & Bouwstra, J. A. (2014). The important role of stratum corneum lipids for the cutaneous barrier function. *Biochimica et Biophysica Acta*, *1841*(3), 295–313. https://doi.org/10.1016/j.bbalip.2013.11.006

Thakoersing, V. S., Gooris, G. S., Mulder, A., Rietveld, M., El Ghalbzouri, A., & Bouwstra, J. A. (2012). Unraveling barrier properties of three different in-house human skin equivalents. *Tissue Engineering. Part C, Methods*, *18*(1), 1–11. https://doi.org/10.1089/ten.TEC.2011.0175

Weterings, P. J., Vermorken, A. J., & Bloemendal, H. (1981). A method for culturing human hair follicle cells. *The British Journal of Dermatology*, *104*(1), 1–5.

Yang, C. C., & Cotsarelis, G. (2010). Review of hair follicle dermal cells. *Journal of Dermatological Science*, *57*(1), 2–11. https://doi.org/10.1016/j.jdermsci.2009.11.005

SUPPORTING INFORMATION

Additional Supporting Information may be found online in the supporting information tab for this article.

Table S1. Primary antibodies for immunofluorescence (IF) and western blot (WB).

Table S2. Primer sequences for qPCR.

Figure S1. (A) A plucked hair follicle in the anagen phase characterized by visible outer root sheath (ORS), inner root sheath (IRS) and hair shaft. (B) Cell outgrowth from the plucked hair follicle at day 7. Arrows indicate spindle-shaped cells potentially indicating the outgrowth of fibroblasts.

Figure S2. Relative mRNA expression levels of (A) type I collagen (*COL1A1*), type IV collagen (*COL4A1*), alpha-smooth muscle actin (*ACTA2*), (B) interleukin-1 alpha (*IL1A*), *IL6*, *IL8* and transforming growth factor-beta (TGF-β*B*) in skin- and hair follicle-derived keratinocytes and fibroblasts. Values are given as mean ± SEM. n = 7–8.

Figure S3. Distinguishing hair follicle-derived fibroblasts (blue) and mouse embryonic firoblasts (green) by real-time duplex PCR. Fluorescence signals were detected in FAM (fluorescence 483–533, human) and YAK (fluorescence 523–568, murine) channels. (A) FAM signal from human DNA but not murine DNA. (B) YAK signal from murine DNA but not human DNA.

Figure S4. Light microscopy of semi-thin sections taken from skin equivalents generated from interfollicular and/or hair follicle-derived cells. The skin equivalents generated from any of the cell combinations displayed all epidermal layers: basal layer (BA), stratum spinosum (SP), stratum granulosum (GR), stratum corneum (CO). Scale bar = 50 μm. n = 3.

Figure S5. (A) Representative hematoxylin & eosin staining (left) and immunostaining against the basal cell marker CK14 (green, middle) and the terminal differentiation marker CK10 (green, right) of human skin biopsies. (B) Representative immunostaining against the skin differentiation markers filaggrin (FLG; green), involucrin (IVL; red) and loricrin (LOR; green) of human skin biopsies. (C) Representative immunostaining against the tight junction proteins occludin (OCLN, green) and claudin 1 (CLDN1, red) of human skin biopsies. (D) Representative immunostaining against the basement membrane proteins type IV collagen (Col IV, red), type VII collagen (Col VII, red) and laminin 5 (LAM5, green) of human skin biopsies. Counterstaining of cell nuclei was performed with 4′,6′-diamin-2-phenylindol (DAPI, blue). Scale bar = 50 μm.

Figure S6. Representative immunostaining against the proliferation marker Ki67 (green) of (A) human skin biopsies and (B) skin equivalents generated from interfollicular and hair follicle-derived cells. Counterstaining of cell nuclei was performed with 4′,6′-diamin-2-phenylindol (DAPI, blue). Scale bar = 100 μm. n = 3.

Figure S7. RNA was isolated from the (A) epidermis and (B) dermis of all generated skin equivalents, transcribed into cDNA, and quantified

by quantitative real-time PCR: relative mRNA expression of involucrin (*IVL*), filaggrin (*FLG*), loricrin (*LOR*), claudin-1 (*CLDN1*), occludin (*OCLN*), type I collagen (*COL1A1*), type III collagen (*COL3A1*), matrix metalloproteinase-2 (*MMP2*) and −9 (*MMP9*) in skin equivalents grown from NHK/NHDF, NHK/HFDF, HFDK/NHDF and HFDK/HFDF. Values are given as mean ± SEM. $n = 3$.

Figure S8. RNA was isolated from the (A) epidermis and (B) dermis of all generated skin equivalents, transcribed into cDNA and quantified by quantitative real-time PCR: type IV collagen (*COL4A1*), type VII collagen (*COL7A1*) and laminin 5 (*LAMA5*). Values are given as mean ± SEM. $n = 3$.

Figure S9. Skin permeability of skin equivalents grown from interfollicular (●) or hair follicle-derived keratinocytes and fibroblasts (○). Values are given as mean ± SEM. $n = 4$.

How to cite this article: Löwa A, Vogt A, Kaessmeyer S, Hedtrich S. Generation of full-thickness skin equivalents using hair follicle-derived primary human keratinocytes and fibroblasts. *J Tissue Eng Regen Med*. 2018;12:e2134–e2146. https://doi.org/10.1002/term.2646